Effects of car wake on performance of low-capacity wind turbine mounted on highways

Minh Duc Le
Faculty of Transportation Mechanical Engineering, The University of Danang- University of Science and Technology

Thanh Dat Phan
Faculty of Transportation Mechanical Engineering, The University of Danang- University of Science and Technology

Shiferaw Regasa Jufar
Department of Petroleum Engineering, Universiti Teknologi PETRONAS

https://doi.org/10.5109/7157970

出版情報：Proceedings of International Exchange and Innovation Conference on Engineering & Sciences (IEICES). 9, pp.188-195, 2023-10-19. 九州大学大学院総合理工学府
バージョン：

Effects of car wake on performance of low-capacity wind turbine mounted on highways

Minh Duc Le[1*], Thanh Dat Phan[1], Shiferaw Regasa Jufar[2]
[1] Faculty of Transportation Mechanical Engineering, The University of Danang− University of Science and Technology, Danang City, Viet Nam
[2]Department of Petroleum Engineering, Universiti Teknologi PETRONAS, Malaysia
*Corresponding author email: minhducle@dut.udn.vn

Abstract: *The effects of car wake on the performance of low-capacity vertical axis wind turbines were studied numerically. A three-blade vertical axis wind turbine (VAWT) was designed to obtain wind energy generated from the car wake. Three VAWTs were mounted on the median strip of a two-lane highway. Computational fluid dynamics was performed to evaluate the performance of wind turbines. The speeds of the car and the distance between the turbines (L) were considered the main factors. The velocity of the car varied in the range of 60 km/h to 120 km/h, while L was operated in 2D, 3D, and 4D. The FFT analysis technique was employed to reveal the car wake characteristics. The car wake significantly affects the performance of turbines interns of revolution and power. The power of a low-capacity VAWT attains a maximum value of about 4.8 W at the velocity of 90 km/h.*

Keywords: Renewable energy; Vertical Axis Wind Turbine (VAWT); Computational Fluid Dynamics (CFD); Vortex Shedding; Fast Fourier Transform (FFT).

1. INTRODUCTION

World energy security is a challenging issue for countries today in terms of specific aspects such as (a) increasing consumption of fossil energy sources, rising fuel costs; (b) depletion of natural resources; (c) the dependence of many countries on supplies from some other resource-rich countries; (d) and environmental hazards that cause global warming. That is why the world needs alternative energy sources for dependence on fossil fuels. Nuclear power and other renewable energy sources, such as wind and solar energy, are alternative energy sources to traditional fuels that do not emit CO_2 into the atmosphere. Among the above energy sources, wind energy does not cause adverse effects on the environment, such as hydroelectric power, which requires deforestation.

High-speed vehicles traveling on highways create a strong turbulence area behind the vehicle and generate a localized form of wind energy [1-2]. The potential of wind energy on highways is very high, considering the long distances and high traffic volume. The small-scale utilization of wind energy by this local wind energy could generate enough electricity to power sensor systems or street lights as well as traffic light signals. Meanwhile, for larger-scale applications, the electricity will be recovered and can be connected to the grid. The idea of recovering energy from the rear vortex formation of vehicles has been studied and proposed before [3-8]. In these studies, Vertical Axis Wind Turbine (VAWT) was used instead of the horizontal axis wind turbine. Wind directions on both sides of the rotor are opposite because of the opposing motion of the vehicles and opposing aerodynamic forces that can drive the rotor [3]. Taskin et al. [5] designed a combined wind and solar energy system to be installed on the highway median. This is a system that uses a multistage Savonius rotor to generate power from the wind when cars pass by Krishnaprasanth et al [3] designed a Maglev turbine for wind power generation on highways. However, these two studies are still in the design process; Numerical or experimental analysis of their design has not yet been conducted. The Savonius turbine [6] and a hybrid wind turbine consisting of a Darrieus rotor and a Savonius rotor [7-8] were designed and tested. These prototype studies demonstrate the feasibility of using wind turbines to generate power from the operation of moving vehicles. However, these tests are simple; No computational or field measurements have been made to demonstrate the practical applicability of these methods, and the mechanism of interaction between the moving vehicle and rotor is unclear.

When a vehicle moves on the road at high speed, it will create large swirls behind the vehicle (i.e., car wake); wind energy from those swirls is a potential source of energy. This energy can be used to generate electrical energy.

In this study, the Vertical Axis Wind Turbine characteristics are investigated for further application on the Vietnam highways system to generate electrical energy when the vehicle crosses the nearby Turbine installation site. Vietnam Expressway is a network of highways extending from north to south and belonging to the Transportation system in Vietnam. The Expressway system in Vietnam consists of individual expressways and sections stretching from north to south. Currently, the maximum vehicle speed on highways in Vietnam is ranged from 80 km/h to 120 km/h [9-10]. The computational simulation is performed to evaluate turbine performance under various operating conditions of vehicle speeds. Turbine operating capacity is evaluated based on the vehicle speed and the distance between turbines.

2. METHODOLOGY

The VAWT is designed to be placed on the median of the highway. Therefore, the wind on both sides of the median will contribute to turbine performance. The wind acting on the blades of the turbine will make the turbine rotate and generate electricity. To evaluate the influence of wake on the VAWT performance, in this study, a numerical simulation will be performed on three wind turbines arranged in tandem for various speeds of cars.

To simplify the calculation model and reduce the calculation time as well as the computer resources, this paper presents the calculation on a 2D model. Many previous studies have demonstrated that using a 2D mathematical model can predict wind turbine performance with good accuracy output [11-12].

The design of the VAWT is shown in Figure 1. The vertical shaft turbine model has three blades with a radius of 125 mm and a blade length of 800 mm [13-15].

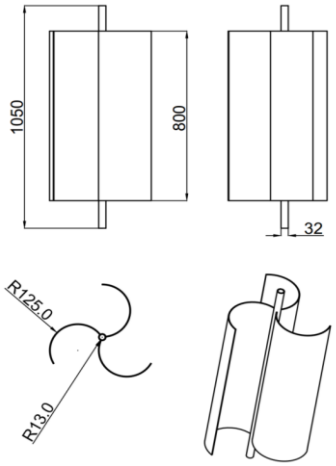

Figure 1. Geometric dimensions of the wind turbine

Within the scope of this study, the vehicle model is the Ahmed simplified car model with a dimension of 4.5 m length × 1.8 m width × 1.5 m height [11]. The influences of different vehicle-body shapes (e.g., cars, trucks, container trucks, etc.) on the VAWT performance will be considered in further studies. According to the Technical standard of roads in Vietnam, the width of the lane is 3.5 m, the width of the median strip is ranged from 0.3 to 0.8 m, and the maximum is 1.27 m. The car speed values used to evaluate the working ability of wind turbines are taken according to the specified car speed limitations on highways in Vietnam. According to this regulation, the maximum allowed speed of cars when traveling in densely populated areas is 60 km/h, the allowed speed of cars outside the densely populated areas is 90 km/h, and the speed of cars allowed to travel on highways is 120 km/h [9-10]. The configuration of wind turbines and cars is presented in Figure 2.

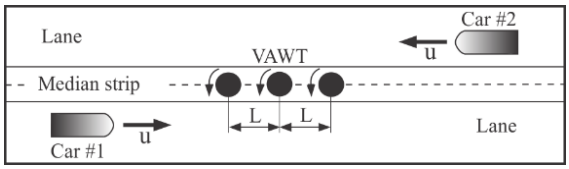

Figure 2. Simulation model of vertical axis wind turbine placed on a two-lane highway in opposite directions

2.1 Geometric Generation

This study analyzes and evaluates the influences of vortex trails on the performance of three Vertical Axis Wind Turbines (VAWTs) under different car speed conditions. The turbines were denoted as T#1, T#2, and T#3. The distance between the VAWTs arranged in tandem was chosen to be equal, i.e., L (as shown in Fig. 3). In this study, three different values of L are employed, i.e., L = 2D, 3D, and 4D (D is the diameter of turbine). The distance from the turbine blade to the car is chosen to be 1 m to correspond to the actual conditions that can ensure safety when the car operates on the road near the median area.

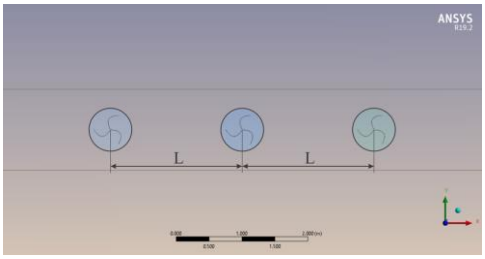

Figure 3. Distance between turbines

2.2 Numerical Model

The influence of car speeds on the operation of vertical axis wind turbines was numerically determined using the commercial software Ansys Fluent R19.2. The computational domain has dimensions of 150 m in length and 15 m in width, which are recommended by Tian et al. [16]. The turbine is located at the center of the domain. The car moves parallel in the *x* direction and is a fixed distance d from the turbine (d = 1m). The position of the car has coordinates (*x*, *y*). The calculation domain is divided into different regions including (a) the turbine rotation region, (b) the car movement region which is a combination of the moving region and the kinematic grid region, (c) and the static region the elements outside the above regions. This configuration is shown in Figure 4.

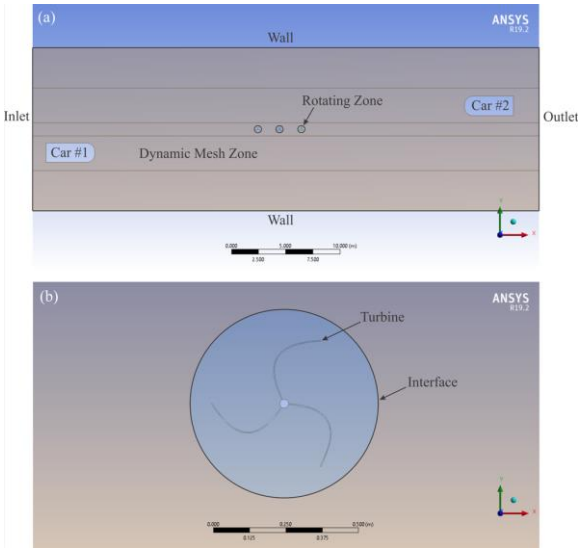

Figure 4. Computational domain and boundary conditions

2.3 Grid Convergence Performance

The computational grid for the model is divided into an unstructured grid (i.e., a triangular grid). The mesh density is more finely divided in the rotational area of the turbine blade system and the region where the car moves. A grid convergence study is carried out to obtain the convergence stage on the calculated results. Three mesh types were performed to evaluate the grid convergence method, i.e., fine mesh, mediate mesh, and coarse mesh with approximately 800,000 elements, 600,000 elements, and 450,000 elements, respectively. A typical instantaneous coefficient of torque (cm) at different mesh qualities at a car speed of 120 km/h was shown in Figure 5. As shown in Figure 5, the mesh quality of fine and

mediate exhibit the same scenario, while the coarse mesh presents a bit lower values compared to others. Finally, the mediate mesh quality was selected to perform the calculations. The details of the calculated grid size are shown in Figure 6.

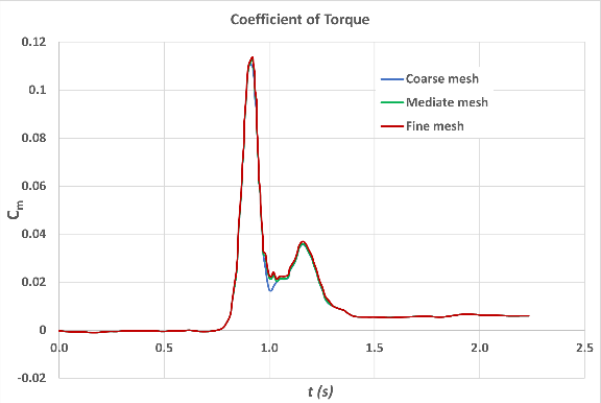

Figure 5. The instantaneous coefficient of torque at different mesh qualities, v = 120 km/h.

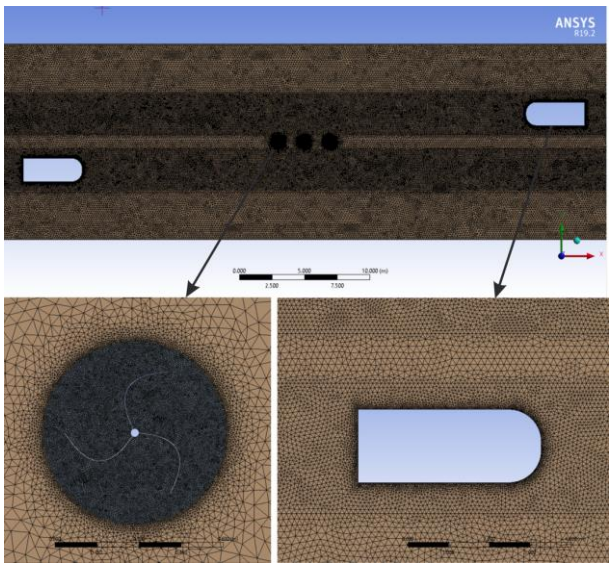

Fig. 6. The detail of mesh.

2.4 Simulation Setup

The *k-ω* shear stress transport (SST) turbulent model is used to calculate as recommended by Tian et al. [16] and Wang et al. [17]. The *k-ω* turbulence model can model the Transfer of turbulent shear stress and provides reliable predictions on the onset and amount of flow separation under unfavorable pressure gradients. The time step is set as 2×10^{-3} s and the displacement of the car at each time step does not go beyond the minimum size in the Transform region of the grid. The Second-Order Upwind algorithm is used for the entire calculation equation including pressure, torque, and turbulence strength. The Least Squares Cell-based algorithm is used for the gradient's operator. The Second-order Algorithms algorithm will give more accurate results than the First-order Algorithms algorithm because it reduces the errors related to interpolation and errors related to error diffusion. Using the above algorithms when conducting simulations with Ansys Fluent software could help satisfy the converge method quickly (Wang et al. 2019; Tian et al. 2015). Three different car speeds of 60, 90, and 120 km/h are performed, while three distances between turbine to turbine (L) of 2D, 3D, and 4D are operated, as shown in Table 1.

Table 1. Simulation cases

Cases	Car speed v, km/h	Distance between turbines L, m
1	60	2D, 3D, 4D
2	90	2D, 3D, 4D
3	120	2D, 3D, 4D

2.5 Validation

Since there are no experiments were previously reported on the effects of car wakes on the VAWTs performance, the validation of the numerical model used in this study was compared to the previous study by Tian et al. [11] in terms of aerodynamics drag coefficient (Cd). The comparison of the Cd is exhibited in Table 2 as follows with a relative error of 1.5%. Therefore, the CFD model can be considered appropriately valid for modeling the effects of car wakes on VAWTs performance.

Table 2. Calculation of coefficient of drag

CASES	Cd
Tian et al. [11]	0.268
Present study	0.272

3. RESULTS AND DISCUSSION

3.1 Vortex Shedding Frequency Analysis

The main parts of the research are (a) estimation of vortices frequency behind the cars and (b) calculation of turbine performance. Flows separated from the car surface and formed a repeating pattern of swirling vortices, similar to the Kármán vortex street. To determine the vortex frequency behind the cars, the Fast Fourier Transform (FFT) was operated to perform a power spectra analysis of the correlation coefficients. The FFT method was applied to vortex shedding from cars at different conditions of speed.

a) One car moving

Figure 7 shows the case of one car moving at various speeds of 60 km/h, 90 km/h, and 120 km/h. The magnitude of the oscillation slightly rises with the increase of the car speed. When the car moves at high speed, the vortex shedding amplitude behind the car is large. The vortex shedding frequency amplitude is shown only at the frequency range from 1 to 50 Hz. As shown in Figure 7, the shedding frequency is increased as increasing the car speeds. For instance, the value of the peak is about 1.2 Hz at a speed of 120 km/h, while it is about 0.8 Hz and 0.91 Hz when the car moves with a speed of 60 km/h and 90 km/h, respectively.

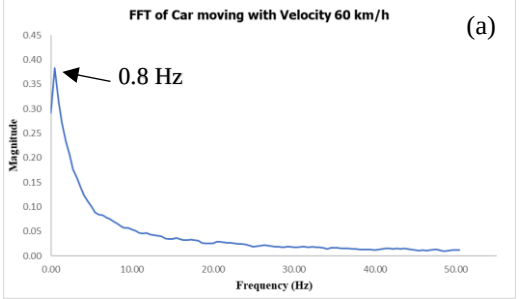

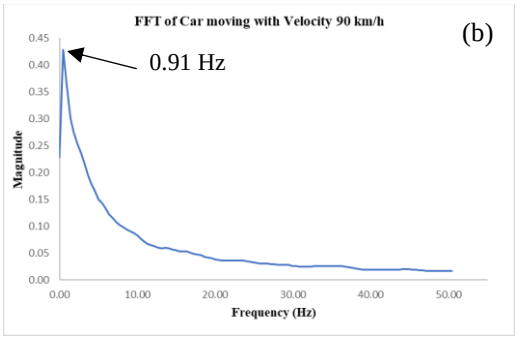

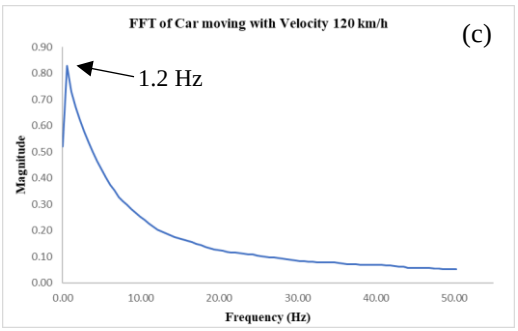

Figure 7. FFT analysis when one car moving at different speeds

b. Two cars moving in the opposite direction

In the case of two cars moving in the opposite direction, as shown in Figure 8, both the length and width of the wake regions behind the cars increase as increasing the speed of the cars. As the car moves, creating separate eddies, the most common eddy structure formed behind the cars is the Kármán vortex. The oscillation of vortex shedding in the case of two cars moving is significantly higher than that in the case of one car moving. The frequency amplitude value is below 50 Hz and increases as increasing the car speed. For instance, as shown in Figures. 8a and 8b, when two cars move with a speed of 60 km/h, the value of peak frequency induced behind the cars is about 0.8 Hz for both Car #1 and Car #2. At a speed of 90 km/h, the peak frequency exhibits at about 1.36 Hz for Car #1 (Fig. 8c), while it is about 1.25 Hz for Car #2 (Fig. 8d). When the cars are moving at a speed of 120 km/h, the oscillating frequency is about 3.84 Hz for both Car #1 and Car#2. Because two cars move in the opposite direction, the vortex Kármán induced in the wakes of the cars is large. Hence, the value of oscillating frequency in the case of two cars is higher than in the case of one car.

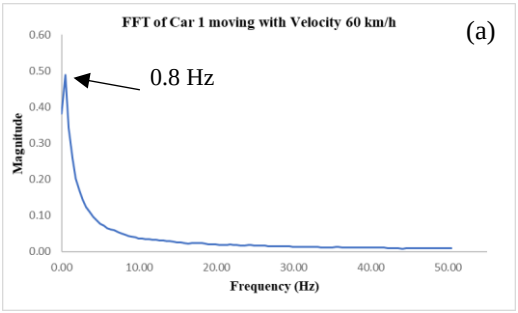

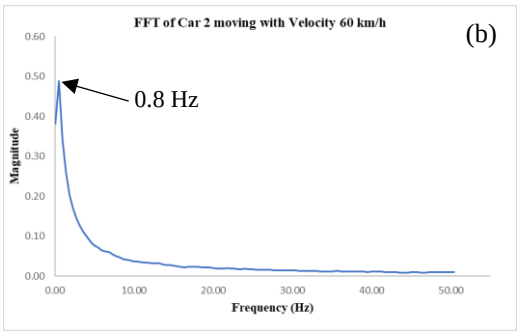

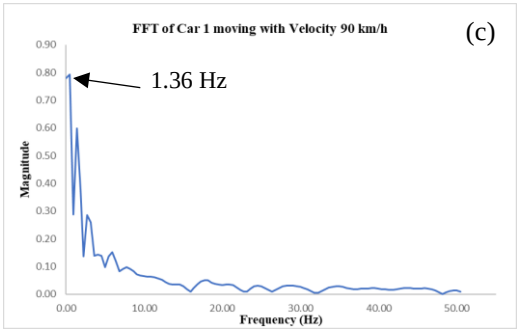

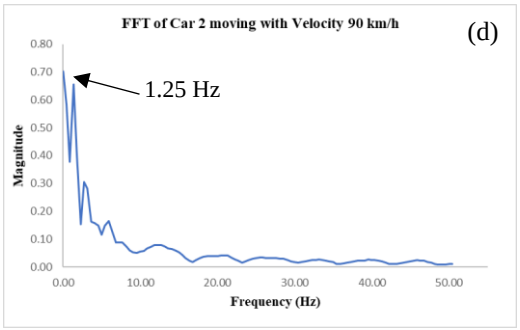

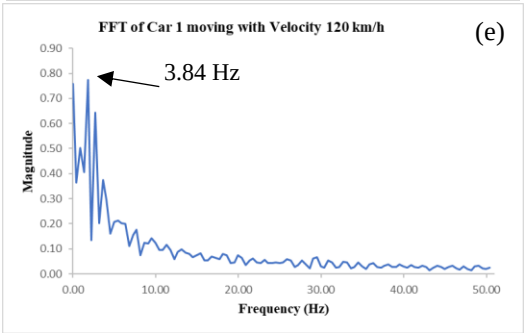

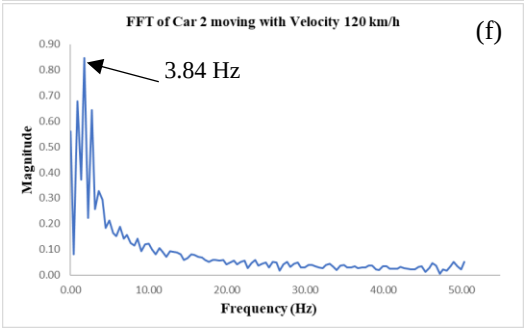

Figure 8. FFT analysis when two cars moving at different speeds

3.2 Influence of the Car Speed on the Performance of Turbine in an Inline Arrangement

a) L = 2D (one car moving)

Figures 9 and 10 show the revolutions and power generated by turbines when only Car #1 is traveling at the

speeds of 60, 90, and 120 km/h. The higher the speed of the car, the greater the intensity of the vortex Kármán Street behind the car, resulting in the turbine being able to generate higher revolutions and more power. In general, as shown in Figure 9, the turbine rapidly generates an increase in the revolution by increasing the car speed from 0.5 s to 1 s. After 1 s and the car speed is above 60 km/h, the revolution of the wind turbine is slightly increased and fluctuated for T#1 and T#2. While it is gradually decreased for T#3. For instance, the maximum value of revolution of VAWT is about 18, 30, and 38 rpm for car speeds of 60, 90, and 120 km/h, respectively.

At a fixed car speed, the revolution gradually increases as the car crossed turbines T#1, T#2, and T#3. For instance, at v = 60 km/h, the maximum value of revolution of T#3 is nearly 12 rpm, while it is about 14 and 18 rpm for T#2 and T#1, respectively. When the car is at 90 km/h, the number of revolutions of T#1 and T#2 increases rapidly compared to those in the case of 60 km/h. For instance, the revolution of T#1 reaches a maximum speed of nearly 30 rpm, while T#2 has a rotational number of 25 rpm. T#3 increases slowly and reaches a maximum speed of nearly 15 rpm. In other words, the revolution of T#1 and T#2 is much higher than that of T#3. This can be explained at the speed of 90 km/h of the vehicle, the effect of the flow through the blades of T#1 and T#2 impeding the movement of T#3, causing T#3 to rotate slowly and emit small capacity. When the car speed is 120 km/h, turbines produce a higher number of revolutions than that at 60 km/h and 90 km/h. In this case, the number of revolutions of T#1 quickly reaches a speed of nearly 40 rpm at 0.8 s. While T#2 has a rotation speed of 35 rpm at 0.8 s; T#3 has a rotation speed of nearly 20 rpm at 0.6 s.
Regarding the revolution of the wind turbine obtained in Figure 9, the power of VAWTs is calculated and shown in Figure 10 as Car #1 crosses the inline arrangement wind turbines. The power of VAWTs is fluctuated along with Time; however, the maximum recorded power is 4 W of T#1 at 0.8 s as Car#1 traveled at 120 km/h. The lower the car speeds, the lower the power of the wind turbine.

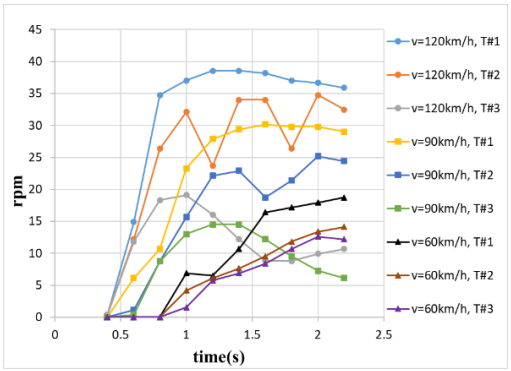

Figure 9. The revolution of turbines

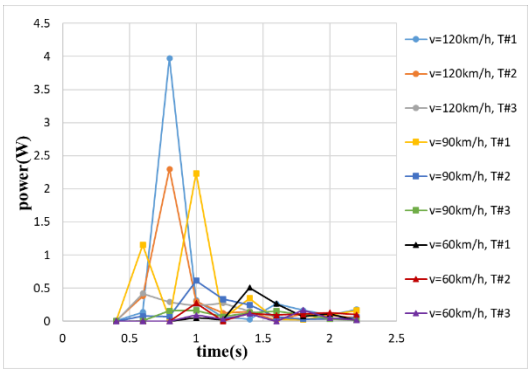

Figure 10. The power of turbines

b) L = 2D (two cars moving in the opposite direction)
When two cars move in the opposite direction and L = 2D, as shown in Figures 11 and 12, the revolution and power of turbines at car speeds of 60, 90, and 120 km/h. When the car's speed is 120 km/h, T#1 has a higher number of revolutions and power than the rest of the cases. For instance, the revolution is about 52 rpm at 1.8 s and the power reaches the maximum value of 2.8W at 1s. When the car speed is 90 km/h, the revolution is about 50 rpm at 2 s and the maximum power is 2.8 W at 1.2 s. At the car speed of 60 km/h, the revolutions and the power of the turbine exhibit relatively low values, e.g., the peak value of the power of T#3 is about 1.4 W at 1.6s.

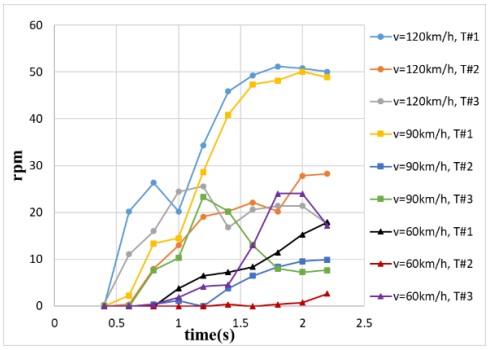

Figure 11. The revolution of turbines

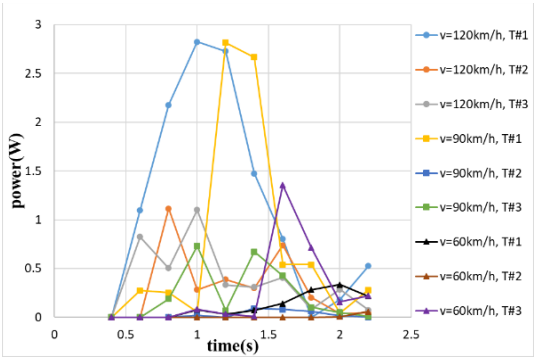

Figure 12. The power of turbines

c) L = 3D (one car moving)

When increasing the distance between turbines to L = 3D, revolutions and power generated by the turbine at the car speeds of 60, 90, and 120 km/h are shown in Fig. 13 and 14, respectively.

At the car speed of 60 km/h, the revolutions and turbine power exhibited the lowest values compared to other car speeds. The revolutions of T#1 reach a peak of 15 rpm at 1.4 s, and the maximum power is about 0.4 W at 1s. The

revolutions of turbines increase slowly over time. When the car is at a speed of 90 km/h, the revolutions and power of the turbine are exhibited a higher value than those in the case of a car speed of 60 km/h. For instance, the revolutions of T#1 reach 20 rpm at 1.2 s, while the power of T#1 attains 0.8 W at 0.6 s.

At the car speed of 120 km/h, T#1 and T#3 have the highest values of revolution and power, while the values of T#2 are exhibited lower. For instance, the maximum power that can be achieved by T#1 and T#3 is about 2.1 W and 3.1 W, respectively, at t = 0.8 s. Whereas, the power of T#2 exhibited a value below 0.5 W. In other words, the capacity of T#1 and T#3 is much higher than the capacity of T#2. This can be explained that at the car speed of 120 km/h, the effect of the flow through the blades of T#1 and T#3 impedes the movement of T#2, causing T#2 to rotate slowly and generate small capacity. The maximum power of the turbine reaches a value of 2.1 W.

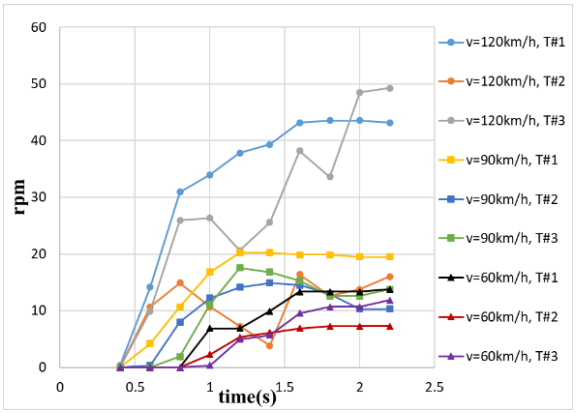

Figure 13. The revolution of turbines

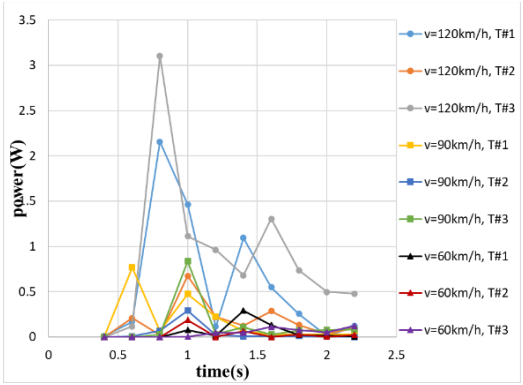

Figure 14. The power of turbines

d) L = 3D (two cars moving in the opposite direction)

Figures 15 and 16 show the revolution and power of turbines when two cars move at the speed of 60, 90, and 120 km/h. The results show that turbines generate the greatest power when two cars are moving in opposite directions because of a large vortex generated behind the car. When the car moves at the speed of 60 km/h, the turbine generates the lowest values of revolution and power. The revolution and power of turbines increase slowly as increasing the car speed. The revolution of T#1 generating nearly 20 rpm and is higher than that of T #2 and T#3. The power of T#1 reaches a peak of 0.8 W at t = 1.8 s. At 90 km/h, the values of revolution and power of the turbine are higher than those in the case of a car speed of 60 km/h. The maximum value of revolution of T#1 reaches 55 rpm at t = 2 s and the power of T#1 attains 4.8W at 1.4s.

At a car speed of 90 km/h, the wake region behind the cars is larger compared to that in the case of one car moving. This results in higher resolution and power than when only one car moves. Therefore, the power of T#1 attains a maximum value of 4.8 W. In the case of 120 km/h, T#2 has a slower increase in revolution compared to the case of T#1 and T#3. This occurred due to the influence of the airflow through turbine blades to impede the movement of T#2. In summary, operating the wind turbines with the distance between turbines as L = 3D can give a higher performance than that in the case of L = 2D.

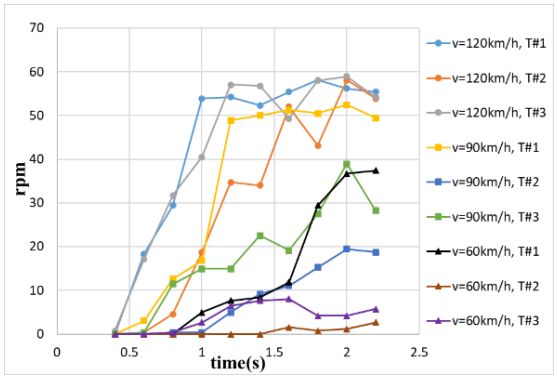

Figure 15. The revolution of turbines

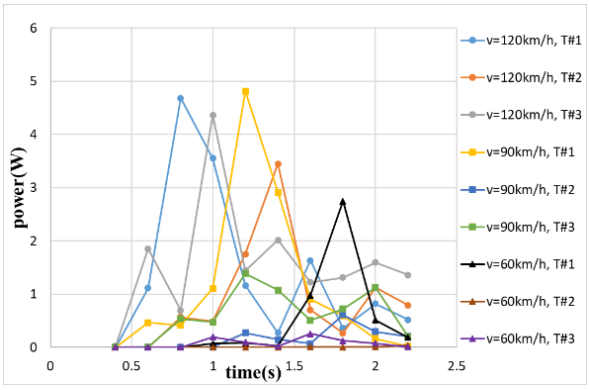

Figure 16. The power of turbines

e) L = 4D (one car moving)

Figures 17 and 18 show the revolutions and power generated by turbines arranged in tandem when the car is traveling at speeds of 60, 90, and 120 km/h. At the car speed of 60 km/h, the revolutions of turbines increase slowly and reach a peak at t = 1.8 s. At 90 km/h, the revolution and power of T#1 and T#2 are higher than those of T#3. The revolution of T#1 reaches 25 rpm at 2 s, while the power reaches 0.8 W at 0.6 s. The revolution of T#2 reaches a peak of 25 rpm at 1.2 s, while the power is 1.5 W at 1s. Therefore, the capacity of T#1 and T#2 is much higher than that of T#3. This can be explained that at the car speed of 90 km/h, the effect of the flow through the blades of T#1 and T#2 impedes the movement of T#3, causing T#3 to rotate slowly and generate a small capacity. T#1 and T#3 have a significantly high revolution and power when the car moves at a speed of 120 km/h. For instance, the revolution of T#1 reaches 48

rpm at 1.6 s, and the power reaches 1.6 W at 1s. While the revolution of T#3 is about 60 rpm at 2 s, and its power reaches 2.3 W at 1.6 s appropriately.

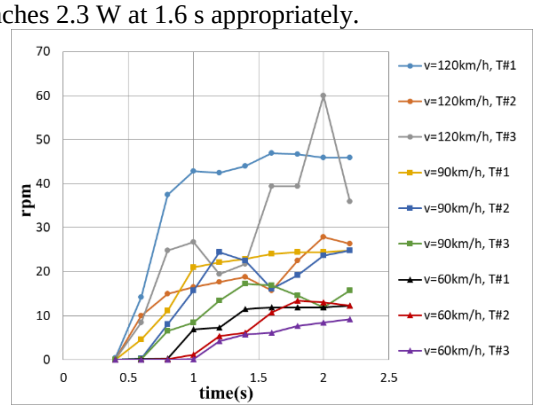

Fig. 17. The revolution of turbines

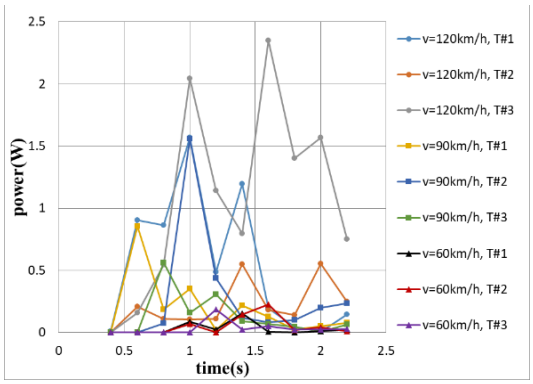

Fig 18. The power of turbines

f) L = 4D (two cars moving in the opposite direction)

As the distance of turbines increases to L = 4 D, the revolution and power generated by turbines when the car moves at 60, 90, and 120 km/h are shown in Figures 19 and 20. The higher the speed of the car, the greater the intensity of the vortex Kármán behind the cars, resulting in the turbine producing a significant increase in revolution and power. When the car speed is at 60 km/h, the turbine exhibits the lowest values in revolution and power. The revolution and power of turbines, in this case, increase slowly with the evolution of time. For instance, the revolutions of T#3 generated nearly 45 rpm higher than T#1, and T#2. The power of T#3 reaches a peak at 2.6 W at t = 1.8 s.

When the car speed is at 90 km/h, the revolution of T#1 and T#3 increases rapidly, and T#1 reaches a maximum value of nearly 70 rpm. T#3 has a rotational number of about 51 rpm, while T#2 increases slowly and only reaches a maximum speed of nearly 25 rpm. Therefore, the capacity of T#1 and T#3 is much higher than that of T#2. This can be explained that at the car speed of 90 km/h, the effect of the flow through the blades of T#1 and T#3 impedes the movement of T#2, causing T#2 to rotate slowly and emit small capacity. The maximum power of the turbine can reach 3.8 W.

At the car speed of 120 km/h, turbines produce a higher value of revolution and power compared to those in the case of 60 km/h and 90 km/h. In this mode, the revolution and turbine power increase rapidly. For instance, T#2 and T#3 have greater revolution and power than T#1. T#2 has a maximum resolution of nearly 62 rpm and a maximum capacity of 4.8 W at 1 s. T#3 has a maximum speed of 55 rpm and a capacity of 4.2 W at 0.8 s. T#1 has a speed of nearly 28 rpm and a power of about 2.3 W at 0.6 s. However, the power of T#1 decreases rapidly after t = 0.6 s. This is because the flow passes through the turbine blades of T#2 and T#3 affecting the operating mode of T#1. This opens a new research direction on the influence of the shaft distance between T#1, T#2, and T#3 in terms of the revolution and the power of turbines.

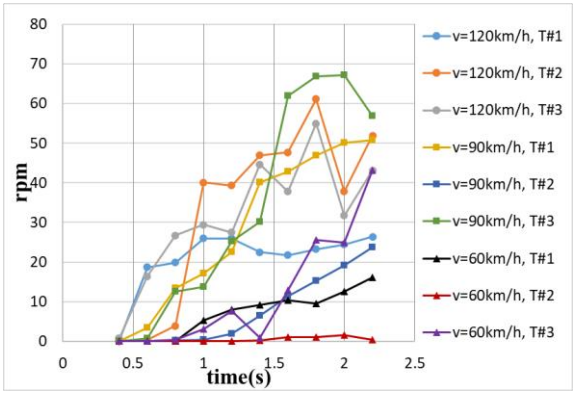

Figure 19. The revolution of turbines

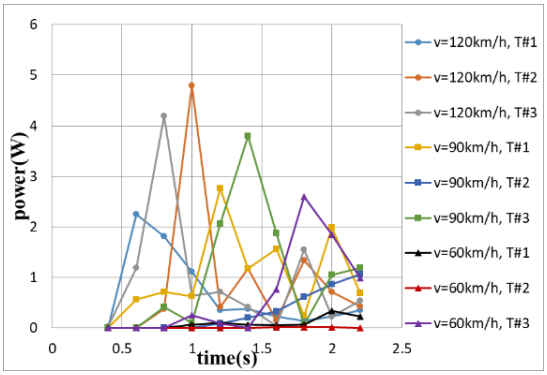

Figure 20. The power of turbines

4. CONCLUSION

In this study, a small-capacity vertical turbine model design was performed numerically. A numerical CFD simulation was carried out to evaluate the revolution and power of turbines at different car speed modes. Some important results of this study may include:

- The turbine rotates at the maximum speed and maximum power when the car moves at a high speed of 90 and 120 km/h. This occurred in the case of three turbines arranged in tandem on the road with L = 1.5 D. T#1 and T#3 have the highest value of revolution and power, while T#2 has a lower number of revolution and power. The maximum power that the turbine produces can reach 4.8 W.
- The turbine generates the most significant power when two cars move in opposite directions because of the large wake induced behind the cars. The car wake generated when passing through is more significant than in the case of only one car moving on the road.
- The wake induced behind the cars is liked a Kármán vortex. The operating mode of the turbine is affected by the oscillations of the repeated Kármán vortices, the number of revolutions as well as the power of the turbine, which fluctuates greatly depending on the frequency of occurrence of these vortices.

- The distance between turbines affects the value of the revolution and the power of the turbines. When L = 4 D, in the case of two cars moving in the opposite direction, T#1 and T#3 provide the highest revolution and power compared to those of T#2. In the case of one car moving, when L = 3D, the revolution and power are significantly higher than those in the other cases of L.

The revolution and power of turbines decrease in proportion to the car's speed, which can be explained by the fact that when the car is moving at a low speed, the Kármán vortex phenomenon induced behind the cars is generated to the side. At low car speeds, the car wake is weaker than that in the case at higher speeds. The results show the renewable energy could be produced from low-capacity VAWTs by recovering energy from automobile wakes at various driving speeds.

5. REFERENCES

[1] Lapointe C. and Gopalan H. (2016). Numerical Investigation of Mini Wind Turbines near Highways. Journal of Solar Energy Engineering, vol.138, no. 2, pp. 1–4.

[2] Rana, Shoel, Biplob Roy, Bidyut Baran Saha, and Sampad Ghosh. "Energy Harvesting from Highway Traffic Vehicles Movement via VAWT." IEICES Proceedings (2022): 122-127.

[3] Krishnaprasanth B., Akshaya P.R., Manivannan L., Dhivya N. (2016). A new-fangled highway wind power generation. International Journal for Research in Applied Science & Engineering Technology, vol. 4, no. 1, pp. 31-34.

[4] Adel, Mohamed, Khalid Hisham, Mahmoud Osama, Adel Awwad, Abdelrahman Mohamed, Amira Elkodama, and Amr Ismaiel. "Twin-Rotor Wind Turbine Power Performance Compared to a Single-Rotor of the Same Tip-to-Tip Spacing." IEICES Proceedings (2021): 323-328.

[5] Taskin S. and Dursun B. (2009). Performance assessment of a combined solar and wind system. Arabian Journal Forence & Engineering, vol. 34, no. 1, pp. 217-27.

[6] Murodiya, R. and H. Naidu (2016). Design and Fabrication of Vertical Wind Turbine for Power Generation at Highway Medians. Int. Eng. J. Res. Dev., Vol. 1 pp. 1-10.

[7] Basilio, M. A., et al. (2019). Harnessing of electrical energy through vehicular air drag on highways for lighting load applications. 2019 IEEE 11th International Conference on Humanoid, Nanotechnology, Information Technology, Communication and Control, Environment, and Management. IEEE.

[8] Champagnie B., Altenor G., Simonis A. (2013). Highway Wind Energy. Florida International University.

[9] Website: Circular 31/2019/TT-BGTVT, issued on August 29, 2019. (accessed 23.06.30).

[10] Website: https://www.invert.vn/danh-sach-cac-tuyen-duong-cao-toc-viet-nam-hien-nay-ar2244. (accessed 23.02.15)

[11] W. Tian, Z. Mao, and Y. Li (2020). Numerical investigation of wind turbines and turbine arrays on highways. Renewable Energy, vol. 147, no. 1, pp. 384-398.

[12] W. Tian, Z. Mao, X. An, B. Zhang, and H. Wen (2017). Numerical study of energy recovery from the wakes of moving vehicles on highways by using a vertical axis wind turbine. Energy, vol. 141, pp. 715-728.

[13] I. Paraschivoiu (2002). Wind turbine design: with emphasis on Darrieus concept. Presses inter Polytechnique.

[14] N.C. Batista, R. Melício, V.M. Mendes, J. Figueiredo, and A. H. Reis (2013). Darrieus wind turbine performance prediction: Computational modeling. Doctoral Conference on Computing, Electrical and Industrial Systems. Springer, Berlin, Heidelberg.

[15] S.R. Shah, R. Kumar, K. Raahemifar, and A.S. Fung (2018). Design, modeling and economic performance of a vertical axis wind turbine. Energy Reports, vol. 4, pp. 619-623.

[16] W. Tian, B. Song, J. H. VanZwieten, P. Pyakurel. (2015). Computational fluid dynamics prediction of a modified Savonius wind turbine with novel blade shapes. Energies, vol. 8, no. 8, pp.7915-7929.

[17] Q. Wang, W. Fang, R. de Richter, C. Peng, T. Ming. (2019). Effect of moving vehicles on pollutant dispersion in street canyon by using dynamic mesh updating method. Journal of Wind Engineering and Industrial Aerodynamics, vol. 187, pp. 15-25.